FULL PAPER

Electromechanics of Ferroelectric-Like Behavior of $LaAlO_3$ Thin Films

Pankaj Sharma, Sangwoo Ryu, Zacharias Viskadourakis, Tula R. Paudel, Hyungwoo Lee, Christos Panagopoulos, Evgeny Y. Tsymbal, Chang-Beom Eom, and Alexei Gruverman**

Electromechanical coupling in complex oxide heterostructures opens new possibilities for the development of a broad range of novel electronic devices with enhanced functionality. In this article, the switchable hysteretic electromechanical behavior of crystalline epitaxial $LaAlO_3$ (LAO) thin films associated with polarization induced by electrical and mechanical stimuli is investigated. The field–time-dependent testing of the induced polarization states along with transport measurements and theoretical modeling suggests that the ferroelectric-like response of the LAO thin films is mediated by the field-induced ion migration in the bulk of the film. Comparative analysis of the dynamics of polarization reversal under the electrical field and mechanical stress applied via a tip of a scanning probe microscope demonstrates that both electrical and mechanical stimulus can be used to effectively control polarization at least at the submillisecond timescale. However, the mechanical writing is more localized than the electrical one. A combined electrical/mechanical approach for tuning the physical properties of oxide heterostructures may potentially facilitate novel memory and logic devices, in which the data bits are written mechanically and read electrically.

1. Introduction

Over the last several years, complex oxide heterostructures and interfaces have become a topic of intense research activity due to the strong coupling between structural, electronic, and spin ordering resulting in a wide spectrum of emerging physical phenomena such as interfacial superconductivity, metal–insulator transitions, strain-driven ferroelectricity, interfacial ferromagnetism, and colossal magnetoresistance.[1] Among the recently discovered effects in complex oxides is the observation of a ferroelectric-like behavior of nominally nonferroelectric materials detected by means of piezoresponse force microscopy (PFM). These materials include $SrTiO_3$,[2–6] TiO_2,[6] amorphous $LaAlO_3$ thin films,[7] $CaCu_3Ti_4O_{12}$,[8] and manganites[9,10] among others with a range of proposed mechanisms for the observed behavior. In the specific case of the $LaAlO_3/SrTiO_3$ (LAO-STO) heterostructures,[11,12] the switchable electromechanical response was attributed either to the field-induced surface charging (as a result of dissociation of water molecules into H^+ and OH^- ions),[12] reversible field-driven redistribution of oxygen vacancies,[11,12] and/or structural distortions at the interface.[13,14] It has been suggested that the switchable PFM response stems for the LAO, rather than the STO layer.[11] Also, it has been recently reported that the polar state of the LAO layers in the LAO-STO heterostructures can be controlled not only by the electrical bias, but also by the tip-induced mechanical force.[15] It is suggested that the strain gradient developed in the LAO film by the tip, pressed against the film surface, generates an internal field much like an applied external voltage, which is likely a result of the flexoelectric effect. In this article, we explore the mechanism of the switchable electromechanical response in the LAO films, and perform comparative studies of the effect of the electrical bias and mechanical pressure on their polar states. We show that the mechanically induced polarization reversal is much more spatially localized and occurs at the submillisecond (ms) timescale, which is comparable with the switching rate of the electrically generated process. The obtained results allow us to establish a correlation between the electrical bias and the tip-induced stress, which

Dr. P. Sharma, Dr. T. R. Paudel,
Prof. E. Y. Tsymbal, Prof. A. Gruverman
Department of Physics and Astronomy
University of Nebraska
Lincoln, NE 68588, USA
E-mail: psharma@unsw.edu.au;
alexei_gruverman@unl.edu
Dr. S. Ryu, Dr. H. Lee, Prof. C.-B. Eom
Department of Materials Science and Engineering
University of Wisconsin-Madison
Madison, WI 53706, USA
Z. Viskadourakis, Prof. C. Panagopoulos
Crete Center for Quantum Complexity and Nanotechnology
University of Crete
Heraklion 71003, Greece
Prof. C. Panagopoulos
Department of Physics
University of Crete and FORTH
Heraklion 71003, Greece
Prof. C. Panagopoulos
Division of Physics and Applied Physics
School of Physical and Mathematical Sciences
Nanyang Technological University
Singapore 637371, Singapore

DOI: 10.1002/adfm.201502483

may prove useful for investigation of the electromechanical coupling in other oxide perovskite materials.

For this study, single-crystalline LAO films (with a thickness of 20 unit cells (u.c.) or ≈7.5 nm) were grown epitaxially on a 10-nm-thick layer of the lattice-matched conducting oxide $Sr_{0.2}Ca_{0.8}RuO_3$ (SCRO) prepared on (001) $(LaAlO_3)_{0.3}$–$(Sr_2AlTaO_3)_{0.7}$ (LSAT) substrate using pulsed laser deposition with in situ monitoring of high pressure reflection high energy electron diffraction (see details in Section I in the Supporting Information). The ferroelectric-like states of the LAO thin films were characterized using a set of scanning probe microscope (SPM) techniques, namely, piezoresponse force microscopy (PFM), electrostatic force microscopy (EFM), and conducting-atomic force microscopy (C-AFM) (Section II, Supporting Information). Pt top electrodes of various diameters (5–150 μm) were deposited using sputtering on the surface of LAO thin films through a hard mask for measurements in capacitor geometry

2. Results and Discussion

LAO thin film surfaces are atomically smooth with single unit-cell high steps clearly visible in atomic force microscopy (AFM) topography image (**Figure 1**a). Local spectroscopic PFM measurements performed at a fixed tip location on a bare LAO surface (Figure 1b) reveal a distinct butterfly-shape nonlinear hysteretic loop for the PFM amplitude signal resembling that observed in classical ferroelectric materials, such as $BaTiO_3$ and Pb $(Zr, Ti)O_3$.[16] The PFM phase loop shows a phase change of ≈180° indicative of reversed electromechanical activity. Further, a pattern consisting of a set of written-in squares was generated on the LAO film surface by scanning it with the electrically biased tip. Bright areas in the PFM phase image (Figure 1d) represent "*in-phase*" electromechanical response of the LAO film to a small sensing ac field (i.e., increase in sample thickness for positive half of the applied ac bias, and decrease in sample thickness for negative half of the applied ac bias cycle) and correspond to the induced polarization oriented downward with negative bound polarization charge on the surface of LAO. Similarly, the dark area in the PFM phase image represents the "*out-of-phase*" response of the upward polarization and corresponds to a positive bound charge on the surface of LAO. The EFM phase image (Figure S2 and Section III, Supporting Information) of the same pattern acquired with a dc read bias of +2 V establishes the presence of a positive surface charge on the areas poled with positive bias, and a negative surface charge on the areas poled with negative bias,[11,17,18] which is opposite to the sign of the bound charge detected in PFM. This confirms that the signals detected in PFM and EFM are unrelated and represent different systems of charges.

To further investigate the surface/bulk nature of the observed electromechanical phenomenon, we deposited Pt top electrodes on the same LAO films, and tested their properties by PFM. In this geometry, where the LAO layer is sandwiched between top and bottom electrodes (**Figure 2**a), the contribution from surface charging/electrostatic effect to the measured PFM signal should be negligible.[19] Local PFM spectroscopic response acquired through the Pt electrode (Figure 2b) again clearly shows the switchable hysteretic behavior, which is further corroborated by the PFM imaging data acquired for the LAO thin film capacitors. In Figure 2c,d, it can be seen that the PFM phase signal of the area under the top electrode changes by ≈180° upon application of the voltage pulses of opposite polarity (±6 V, 1 s). These results rule out the surface charging effect and confirm the bulk character of the observed ferroelectric-like response in the LAO films.

To probe the possible contribution of direct charge injection to the PFM signal, we measured local spectroscopic current–voltage (*I*–*V*) curves on the LAO films via C-AFM. It was found that (Figure S3 and Section IV, Supporting Information) the current injection is extremely low for biases below 7.5 V. The fact that the switchable hysteretic behavior is observed at biases below 6 V, where current injection is significantly limited, rules out current injection as being the origin of switchable electromechanical response.[7] Bulk electrochemical processes, such as cationic demixing associated with irreversible material degradation, were not observed within the bias window of ±6 V over which the LAO films exhibit a hysteretic PFM response.[12] Moreover, the observed relaxation of the electrically written states (Figure S4 and Section V, Supporting Information) indicates the absence of stable polarization as the equilibrium thermodynamic ground

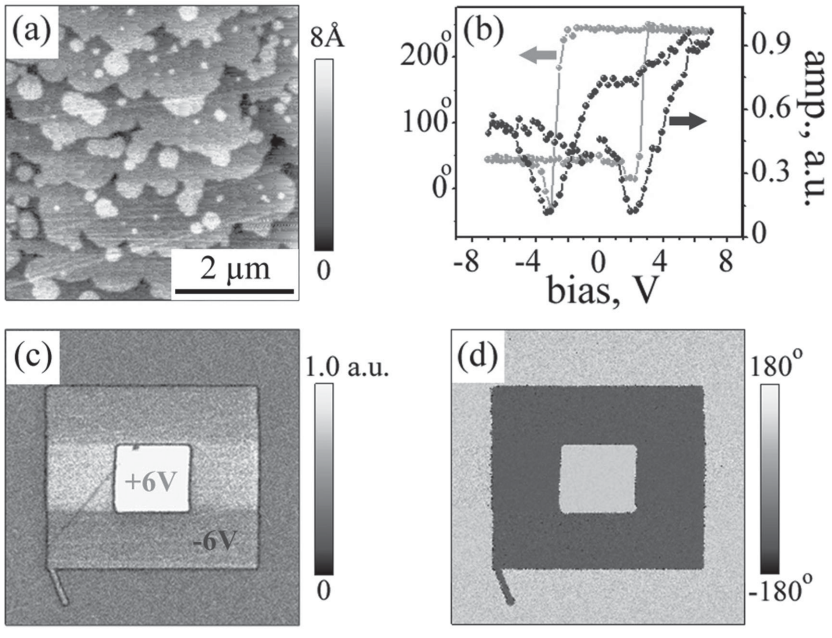

Figure 1. Electromechanical behavior of the LAO (20 u.c.)/SCRO (10 nm)/LSAT heterostructure. a) Topography image of the LAO surface. b) Local spectroscopic PFM amplitude and phase hysteresis loops. c) PFM amplitude and d) the corresponding phase images of the LAO film after electrical poling first by –6 V (the outer square of 3 × 3 μm^2) and then by + 6 V (the inner square of 1 × 1 μm^2).

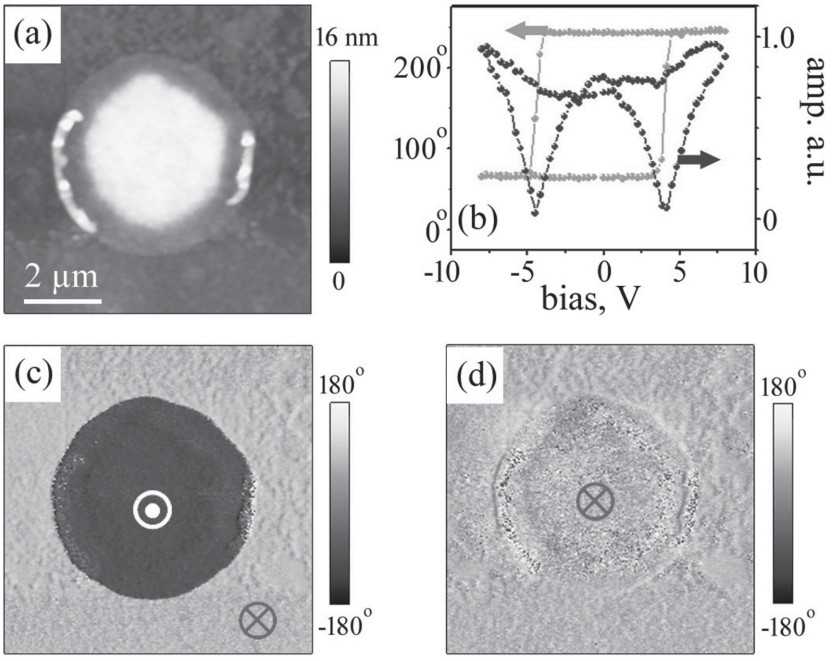

Figure 2. Electromechanical response through the top electrode. a) Topography image showing Pt top electrode on the LAO film. b) Local spectroscopic PFM amplitude and phase hysteresis loops acquired through the top metal electrode. c) PFM phase images acquired after application of (–6 V, 1s) pulse and d) after application of (+6 V, 1s) pulse, respectively, to the Pt top electrode.

state and shows a behavior reminiscent to that of electrets, where polarization is induced by a metastable separation of ionic charge/charged defects rather than by a stable long-range dipolar orientation.

With several possible mechanisms being ruled out, we suggest that the bistable distribution of ions/oxygen vacancies introduced during the film growth[20,21] is the origin of the switchable PFM response. First-principles calculations of the oxygen vacancy formation energy support such a mechanism in $LaAlO_3/SrRuO_3$ (LAO/SRO) heterostructures (**Figure 3**a). Theoretical results (details are given in Section VI in the Supporting Information) predict a bistable distribution of oxygen vacancies (Figure 3b). The uncompensated electric field in a polar LAO film results in a linear reduction of the electrostatic potential creating a minimum in the oxygen vacancy formation energy at the LAO surface. On the other hand, the interfacial charge formed in metallic SRO to screen the polarization of LAO produces an electric field in SRO leading to a decrease in the electrostatic potential and the oxygen vacancy formation energy when moving from the LAO/SRO interface to the bulk SRO. Application of a positive or negative external bias causes reversible movement of oxygen vacancies between the two energy minima across the potential barrier at the LAO/SRO interface producing the observed switchable and stable piezoresponse behavior. Additionally, application of a relatively low bias to the AFM tip can generate sufficiently high electric fields to inject or remove oxygen vacancies.[6,12]

To test the feasibility of the mechanism based on field-assisted ion dynamics, we studied the field–time dependence of the written domains in LAO thin films. A 4 × 4 matrix (Figure 3c,d) of locally poled areas (resembling ferroelectric domains) has been produced by application of voltage pulses of varying amplitude (from 4 V to 10 V) and duration (from 10 s to 120 s) using the conductive AFM tip. As can be seen (Figure 3c,d; Figure S5, Supporting Information), circular domains with reversed electromechanical response grow larger with stronger and longer pulses. Note that in the ferroelectric thin films domains of similar or even bigger sizes can be created by application of much shorter pulses at similar or even smaller tip-generated fields (e.g., domains of ≈200 nm in diameter can be produced by 6 V, 1 s pulse in 60 nm thick $BaTiO_3$ films.[22] This is indicative of the different switching mechanisms in ferroelectric films (mediated by nucleation, forward growth, and sideways movement of the domain walls[23–25] and LAO films. Since the ionic species are usually characterized by rather large diffusion times,[26] the much slower sideways expansion of the poled areas in the LAO

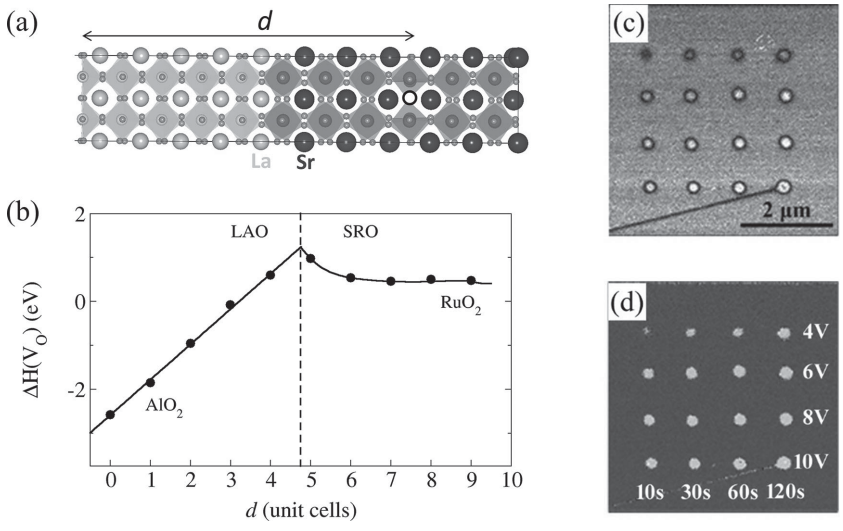

Figure 3. First-principles calculations and scaling of the electromechanical response. a) Atomic structure of an LAO/SRO system used in first-principles calculations. The oxygen vacancy (V_O) shown in black circle lies at distance *d* away from the LAO surface. b) Formation energy of oxygen vacancies as a function of distance *d* from the LAO surface (where $d = 0$) in the LAO/SRO heterostructure. The black solid circles are actual calculated data, and the solid line is a guide to the eye. The dashed line indicates schematically the LAO/SRO interface. c) PFM amplitude and d) the corresponding PFM phase image, obtained in PFM mode after creation of the dot pattern by application of pulses of various amplitude and duration.

films is consistent with a model based upon field-assisted ion dynamics as the origin of their ferroelectric-like behavior.

It is well established that the field-induced ion migration can result in resistive switching effects.[27–30] The resistive switching behavior reported for the LAO/STO interfaces[29] is attributed, among other mechanisms, to the external field induced drift of oxygen vacancies. This mechanism is also consistent with the field-assisted ion-migration model of the ferroelectric-like behavior of the LAO thin films. To probe their resistive properties, we performed out-of-plane transport measurements in the LAO thin film capacitors (details are given in Section VIII in the Supporting Information). A rather small ON/OFF resistance ratio (≈3) allows us to rule out the formation of highly conducting channels (filaments).[30] It can be argued that the field-assisted reorganization of oxygen vacancies creates an asymmetric potential profile across the LAO layer resulting in the resistive switching effect. We note that additional studies are necessary to further corroborate the mechanism of the resistive switching behavior (interface vs the bulk effect).

Next, we investigated the effect of mechanical pressure on the electromechanical response of the LAO thin films. In this experiment, a grounded AFM tip is pressed against the sample surface exerting a mechanical force, which affects the polar state of the LAO film. To visualize the effect of tip-induced mechanical pressure, first a bidomain state was created by an electrical prepoling of the LAO surface. Then, a 1×1 μm^2 area within this electrically prepatterned region (shown by the dashed-line frame in **Figure 4**a,b) was scanned with an incrementally increasing tip-induced loading force (in the bottom up direction). The subsequent PFM maps (Figure 4a,b) acquired under a low loading force (≈50 nN) show a transition from the upward to the downward polarization state occurring at a threshold load of ≈950 nN. This transition is marked by a phase shift of ≈180° and nearly a zero amplitude in the PFM phase and amplitude images, respectively. (Note that topographic imaging performed after application of the mechanical force shows no visible damage to the surface of LAO film; Figure S7 and Section IX in the Supporting Information). In other words, application of mechanical pressure via the SPM tip flips the polar state of the LAO film in the same way as the application of the positive bias to the tip. This behavior is similar to that observed in ferroelectric thin films and LAO-STO heterostructures.[15,31] The electric field caused by the SPM tip pressure could arise from the flexoelectric effect present in all crystalline materials. As shown recently, a strain gradient generated in thin films can be huge[31,32] and can cause internal electric fields large enough to drive polarization reversal.

We have calibrated the mechanical force in terms of a bias voltage that generates an electric field of equivalent strength. We adopted an approach, in which the tip is electrically biased with a small positive DC offset as it is scanned exerting incrementally increasing loading force over an electrically prepoled region (using −6 V bias) of the LAO surface. Thereafter, PFM images were acquired and were used to determine the threshold loading force value for different DC bias offsets. A positive DC bias applied to the tip results in an electric field aligned in the same direction as the flexoelectric field generated by the loading force, and therefore, the threshold load needed to mechanically switch the PFM signal decreases (Figure 4c). A linear fit to the obtained data establishes a bias–load conversion factor of ≈2.3 V μN^{-1} (Figure 4d). The obtained value is in good agreement with the value of 2.1 V μN^{-1} estimated from the direct comparison of local coercive bias of ≈2 V (found from the PFM loop in Figure 1b), and the threshold loading force of ≈950 nN determined from the PFM maps in Figure 4a,b. The mechanically written states are still responsive to an electrical stimulus (Figure S8 and Section X, Supporting Information).

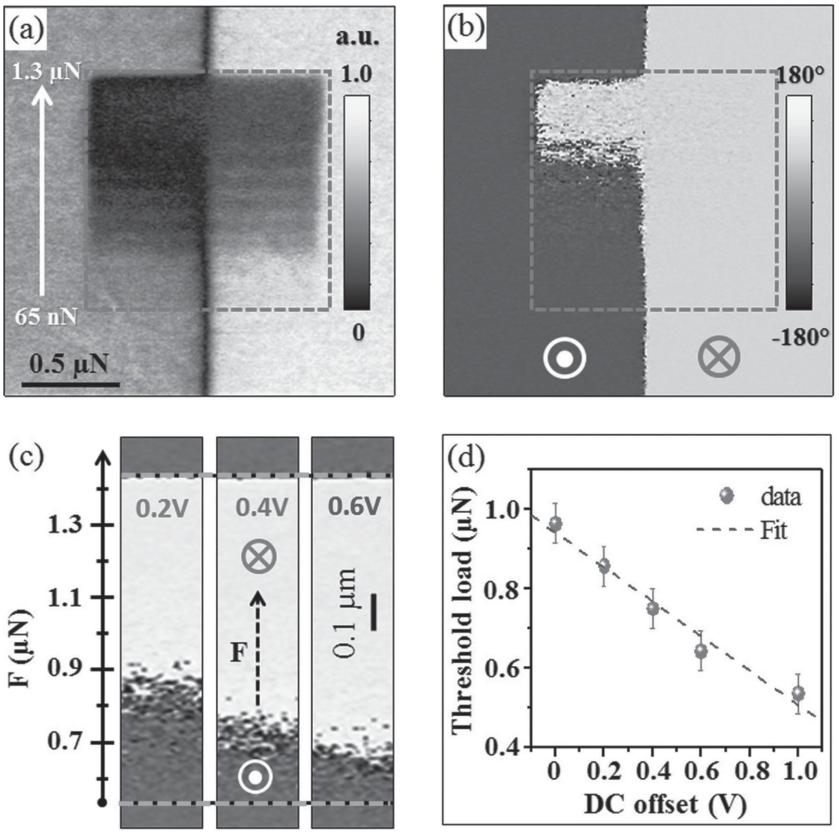

Figure 4. Mechanical reversal of the polar states. a) PFM amplitude and b) the corresponding phase image, after a 1×1 μm^2 area in the center (denoted by a dashed-line frame) has been scanned with the tip under an incrementally increasing loading force. c) PFM phase images obtained after scanning with an incrementally increasing loading force (scale shown on left of images) within the dotted green lines, while the tip was maintained at a certain variable dc bias (indicated on the respective image). d) Plot of thresold loading force versus positive DC offset on the tip during scanning with the increasing mechanical force. Dashed-line frame in a,b) marks the area where incrementally increasing loading force (from 67 nN to 1.3 μN) was applied. Dotted line in d) indicates the linear fit to the data.

To compare the rate at which the ferroelectric-like response of the LAO films can be reversed using electrical or mechanical means, two patterns consisting of linear polar regions were written at various tip scanning velocities (from several nm s^{-1} to μm s^{-1}) (**Figure 5**a,b). The first pattern consists of the lines written in the contact mode at a nominally low loading force (≈50 nN) with the tip at a DC bias of +3.5 V, which is above the coercive voltage. The second pattern is comprised of lines written with the electrically grounded tip, which scanned the surface under a mechanical load equivalent to the 3.5 V bias as determined from Figure 4d (about 1.5 μN). Depending upon the scanning rate, the tip dwell time at each pixel (with the size of about 4×4 nm^2) ranged from ≈4 s (1 nm s^{-1}) to 0.2 ms (20 μm s^{-1}). From the PFM images in Figure 5a,b (see also Figures S9 and S10 in Section XI in the Supporting Information), it is evident that both the electrical and mechanical stimulus can be used to effectively control the polar state of the LAO films at the submillisecond timescale. Notably, the switching speed in the mechanical mode is limited by our experimental setup and the intrinsic speed for the mechanically induced switching could be much higher.[32]

From comparison of the width of the mechanically and electrically written linear polar regions (Figure 5c), it can be concluded that the mechanically written regions are more localized than the electrically induced ones for the tip scanning velocities below 200 nm s^{-1}. Above this value the difference between the electrically and mechanically written lines becomes indistinguishable within the PFM imaging resolution. From Figure 5c, it can also be deduced that mechanical switching occurs at a lower rate in comparison with the electrical switching, which is again a manifestation of the localized nature of the elastic fields generated by the tip pressure. This localization arises from a much smaller volume over which a mechanical stress is exerted by the tip, in contrast to the volume affected by the electric field, which extends over distances well beyond the tip-sample contact area, which is of the order of 10 nm. In turn, the flexoelectric field associated with the tip-induced strain gradient decays much faster with the distance from the tip. This results in slower mechanical switching at distances much larger than 10 nm. Hence, the data presented in Figure 5c, first, indirectly support the flexoelectric mechanism of the mechanical switching, and, second, indicate essentially different length scales of the electrical and elastic fields.

3. Conclusions

In summary, electrically and mechanically induced ferroelectric-like polar states of the LAO films were characterized using

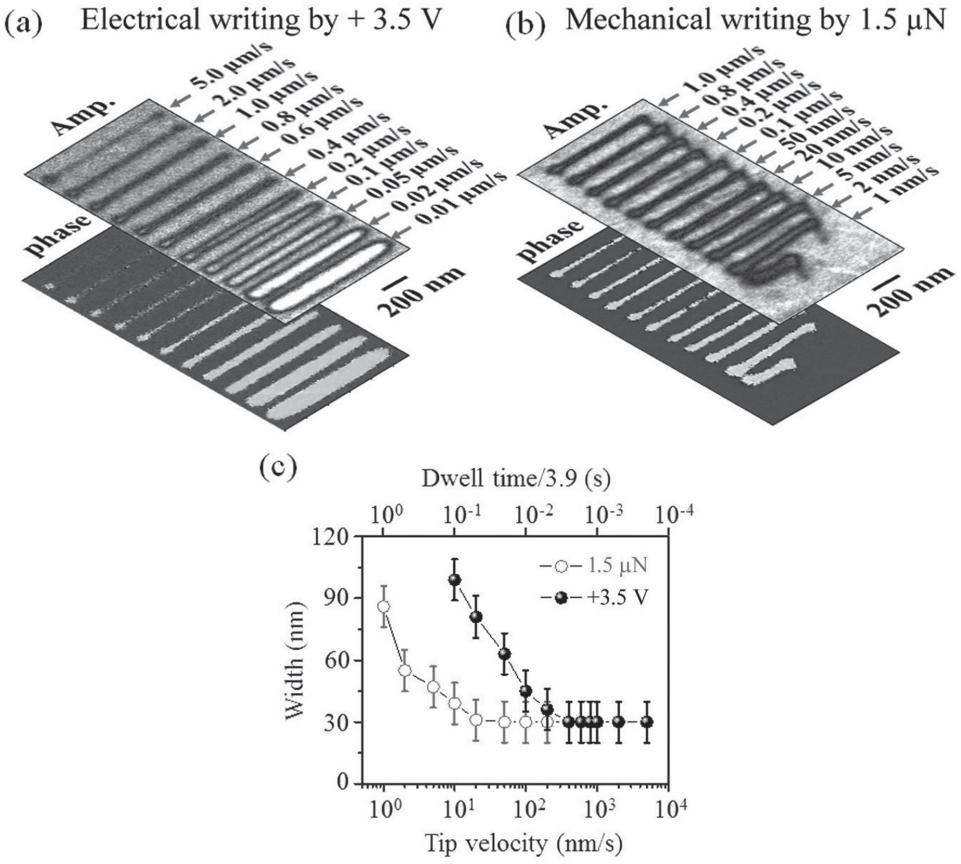

Figure 5. Comparison of electrical and mechanical writing. a) PFM amplitude (top) and phase images (bottom), respectively, obtained after writing lines electrically by scanning in contact mode at different speeds (as indicated) using an AFM tip held at a DC bias of +3.5 V. b) PFM amplitude (top) and phase images (bottom), respectively, obtained after writing lines mechanically by scanning in contact mode at different speeds (as indicated) using an AFM tip exerting a loading force of ≈1.5 μN. c) Plot of the width of the lines written electrically and mechanically as a function of tip velocity (or the dwelling time).

a combination of SPM techniques. Comparative analysis of the effect of electrical and mechanical stimuli on the polar states in $LaAlO_3$ along with the transport measurements allowed us to establish a correlation between the electrical bias and the tip-induced stress and attribute the ferroelectric-like response of the $LaAlO_3$ thin films to the ion migration in the bulk of the film. This mechanism is presumably associated with the reorganization of oxygen vacancies between the two stable states, which can be controlled at the sub-millisecond timescale using either the electrical or the mechanical stimulus. The mechanical control of the polar states was found to be more localized than the one by electrical means.

The obtained results demonstrate an exciting possibility of replication of the ferroelectric functionality in nominally non-ferroelectric materials. In addition, this outcome may prove useful for investigation of the mechanism of electromechanical coupling in other complex oxide materials. Further studies of ion dynamics in oxide heterostructures/interfaces will open new opportunities for tuning the physical properties of oxide-based electronic devices via a combined electromechanical approach thereby facilitating novel memory and logic applications, in which the data is written mechanically and read electrically.

Supporting Information

Supporting Information is available from the Wiley Online Library or from the author.

Acknowledgements

This work was mainly supported by the US Department of Energy, Office of Science, Basic Energy Sciences, Division of Materials Sciences and Engineering, under Award DE-SC0004876 (scanning probe measurements). Electrical measurements and modeling at the University of Nebraska-Lincoln were supported by the National Science Foundation (NSF) through the Nebraska Materials Research Science and Engineering Center (MRSEC) under Grant No. DMR-1420645. Design and fabrication of thin film heterostructures at the University of Wisconsin-Madison was supported by the NSF grant DMR-1234096 and the AFOSR grant FA9550-12-1-0342. First-principles calculations were performed at the University of Nebraska Holland Computing Center. The work in Greece was partially supported by the European Union's Seventh Framework Program (FP7-REGPOT-2012-2013-1) under grant agreement no. 316165, the European Social Fund (ESP), and Greek national funds through the Operational Program "Education and Lifelong Learning" of the National Strategic Reference Framework (NSRF) under "Funding of proposals that have received a positive evaluation in the third and fourth Call of ERC Grant Schemes." The work in Singapore was supported by the National Research Foundation, Singapore, through Grant NRF-CRP4-2008-04.

Received: June 18, 2015
Revised: July 31, 2015
Published online: September 24, 2015

[1] E. Y. Tsymbal, E. R. A. Dagotto, C. B. Eom, R. Ramesh, *Multifunctional Oxide Heterostructures*, Oxford University Press, Oxford, UK, **2012**.
[2] J. H. Haeni, P. Irvin, W. Chang, R. Uecker, P. Reiche, Y. L. Li, S. Choudhury, W. Tian, M. E. Hawley, B. Craigo, A. K. Tagantsev, X. Q. Pan, S. K. Streiffer, L. Q. Chen, S. W. Kirchoefer, J. Levy, D. G. Schlom, *Nature* **2004**, *430*, 758.
[3] M. P. Warusawithana, C. Cen, C. R. Sleasman, J. C. Woicik, Y. Li, L. F. Kourkoutis, J. A. Klug, H. Li, P. Ryan, L.-P. Wang, M. Bedzyk, D. A. Muller, L. Q. Chen, J. Levy, D. G. Schlom, *Science* **2009**, *324*, 367.
[4] A. Vasudevarao, A. Kumar, L. Tian, J. H. Haeni, Y. L. Li, C.-J. Eklund, Q. X. Jia, R. Uecker, P. Reiche, K. M. Rabe, L. Q. Chen, D. G. Schlom, V. Gopalan, *Phys. Rev. Lett.* **2006**, *97*, 257602.
[5] A. Kholkin, I. Bdikin, T. Ostapchuk, J. Petzelt, *Appl. Phys. Lett.* **2008**, *93*, 222905.
[6] Y. Kim, A. N. Morozovska, A. Kumar, S. Jesse, E. A. Eliseev, F. Alibart, D. Strukov, S. V. Kalinin, *ACS Nano* **2012**, *6*, 7026.
[7] A. S. Borowiak, N. Baboux, D. Albertini, B. Vilquin, G. S. Girons, S. Pelloquin, B. Gautier, *Appl. Phys. Lett.* **2014**, *105*, 012906.
[8] R. Tararam, I. Bdikin, N. Panwar, J. A. Varela, P. R. Bueno, A. Kholkin, *J. Appl. Phys.* **2011**, *110*, 052019.
[9] R. F. Mamin, I. K. Bdikin, A. L. Kholkin, *Appl. Phys. Lett.* **2009**, *94*, 222901.
[10] F. G. N. Figueiras, I. K. Bdikin, V. B. S. Amaral, A. L. Kholkin, *Phys. Chem. Chem. Phys.* **2014**, *16*, 4977.
[11] C. W. Bark, P. Sharma, Y. Wang, S. H. Baek, S. Lee, S. Ryu, C. M. Folkman, T. R. Paudel, A. Kumar, S. V. Kalinin, A. Sokolov, E. Y. Tsymbal, M. S. Rzchowski, A. Gruverman, C. B. Eom, *Nano Lett.* **2012**, *12*, 1765.
[12] A. Kumar, T. M. Arruda, Y. Kim, I. N. Ivanov, S. Jesse, C. W. Bark, N. C. Bristowe, E. Artacho, P. B. Littlewood, C.-B. Eom, S. V. Kalinin, *ACS Nano* **2012**, *6*, 3841.
[13] M. Huang, F. Bi, S. Ryu, C.-B. Eom, P. Irvin, J. Levy, *APL Mater.* **2013**, *1*, 052110.
[14] M. Huang, F. Bi, C.-W. Bark, S. Ryu, K.-H. Cho, C.-B. Eom, J. Levy, *Appl. Phys. Lett.* **2014**, *104*, 161606.
[15] P. Sharma, S. Ryu, J. D. Burton, T. R. Paudel, C. W. Bark, Z. Huang, Ariando, E. Y. Tsymbal, G. Catalan, C. B. Eom, A. Gruverman, *Nano Lett.* **2015**, *15*, 3547.
[16] A. Gruverman, A. Kholkin, *Rep. Prog. Phys.* **2006**, *69*, 2443.
[17] Y. Xie, C. Bell, T. Yajima, Y. Hikita, H. Y. Hwang, *Nano Lett.* **2010**, *10*, 2588.
[18] Y. Xie, C. Bell, Y. Hikita, H. Y. Hwang, *Adv. Mater.* **2011**, *23*, 1744.
[19] D. A. Bonnell, S. V. Kalinin, A. Kholkin, A. Gruverman, *MRS Bull.* **2009**, *34*, 648.
[20] A. Brinkman, M. Huijben, M. van Zalk, J. Huijben, U. Zeitler, J. C. Maan, W. G. van der Wiel, G. Rijnders, D. H. A. Blank, H. Hilgenkamp, *Nat. Mater.* **2007**, *6*, 493.
[21] G. Herranz, M. Basletic, M. Bibes, C. Carre´te´ro, E. Tafra, E. Jacquet, K. Bouzehouane, C. Deranlot, A. Hamzic, J. M. Broto, A. Barthelemy, A. Fert, *Phys. Rev. Lett.* **2007**, *98*, 216803.
[22] N. A. Pertsev, A. Petraru, H. Kohlstedt, R. Waser, I. K. Bdikin, D. Kiselev, A. L. Kholkin, *Nanotechnology* **2008**, *19*, 375703.
[23] J. F. Scott, in *Ferroelectric Random Access Memories: Fundamentals and Applications* (Eds: H. Ishiwara, M. Okuyama, Y. Arimoto), Springer-Verlag, Berlin, Germany **2004**.
[24] J. Li, B. Nagaraj, H. Liang, W. Cao, Chi. H. Lee, R. Ramesh, *Appl. Phys. Lett.* **2004**, *84*, 1174.
[25] Y. Ehara, S. Yasui, J. Nagata, D. Kan, V. Anbusathaiah, T. Yamada, O. Sakata, H. Funakubo, V. Nagarajan, *Appl. Phys. Lett.* **2011**, *99*, 182906.
[26] S. Zafar, H. Jagannathan, L. F. Edge, D. Gupta, *Appl. Phys. Lett.* **2011**, *98*, 152903.
[27] K. Szot, W. Speier, G. Bihlmayer, R. Waser, *Nat. Mater.* **2006**, *5*, 312.
[28] Y. B. Nian, J. Strozier, N. J. Wu, X. Chen, A. Ignatiev, *Phys. Rev. Lett.* **2007**, *98*, 146403.

[29] S. Wu, X. Luo, S. Turner, H. Peng, W. Lin, J. Ding, A. David, B. Wang, G. V. Tendeloo, J. Wang, T. Wu, *Phys. Rev. X* **2013**, *3*, 041027.
[30] R. Waser, R. Dittmann, G. Staikov, K. Szot, *Adv. Mater.* **2009**, *21*, 2632.
[31] H. Lu, C.-W. Bark, D. Esque de los Ojos, J. Alcala, C. B. Eom, G. Catalan, A. Gruverman, *Science* **2012**, *336*, 59.
[32] P. M. Solomon, B. A. Bryce, M. A. Kuroda, R. Keech, S. Shetty, T. M. Shaw, M. Copel, L.-W. Hung, A. G. Schrott, C. Armstrong, M. S. Gordon, K. B. Reuter, T. N. Theis, W. Haensch, S. M. Rossnagel, H. Miyazoe, B. G. Elmegreen, X.-H. Liu, S. Trolier-McKinstry, G. J. Martyna, D. M. Newns, *Nano Lett.* **2015**, *15*, 2391.